Hypothalamic Ahi1 Mediates Feeding Behavior through Interaction with 5-HT$_{2C}$ Receptor*[S]

Hao Wang[‡1], **Zhenbo Huang**[‡1], **Liansha Huang**[§1] **Shaona Niu**[¶], **Xiurong Rao**[‡], **Jing Xu**[‡], **Hui Kong**[‡], **Jianzhong Yang**[∥], **Chuan Yang**[**], **Donghai Wu**[‡], **Shihua Li**[‡‡], **Xiao-Jiang Li**[‡‡], **Tonghua Liu**[§2], and **Guoqing Sheng**[‡3]

From the ‡*CAS Key Laboratory of Regenerative Biology, South China Institute for Stem Cell Biology and Regenerative Medicine, Guangzhou Institutes of Biomedicine and Health, Chinese Academy of Sciences, Guangzhou 510530, China, the* §*Department of Science and Technology, Beijing University of Chinese Medicine, Beijing 100029, China, the* ¶*Department of Endocrinology, Linyi People's Hospital, 27 Jiefang Road, Linyi 276003, China, the* ∥*Red Cross Hospital of Yunnan Province, Kunming 650030, China, the* **Department of Endocrinology and Metabolism, The Second Affiliated Hospital of Sun Yat-sen University, Guangzhou 510020, China, and the* ‡‡*Department of Human Genetics, Emory University School of Medicine, Atlanta, Georgia 30322*

It is indicated that there are important molecules interacting with brain nervous systems to regulate feeding and energy balance by influencing the signaling pathways of these systems, but relatively few of the critical players have been identified. In the present study, we provide the evidence for the role of Abelson helper integration site 1 (Ahi1) protein as a mediator of feeding behavior through interaction with serotonin receptor 2C (5-HT$_{2C}$R), known for its critical role in feeding and appetite control. First, we demonstrated the co-localization and interaction between hypothalamic Ahi1 and 5-HT$_{2C}$R. Ahi1 promoted the degradation of 5-HT$_{2C}$R through the lysosomal pathway. Then, we investigated the effects of fasting on the expression of hypothalamic Ahi1 and 5-HT$_{2C}$R. Fasting resulted in an increased Ahi1 expression and a concomitant decreased expression of 5-HT$_{2C}$R. Knockdown of hypothalamic Ahi1 led to a concomitant increased expression of 5-HT$_{2C}$R and a decrease of food intake and body weight. Last, we found that Ahi1 could regulate the expression of neuropeptide Y and proopiomelanocortin. Taken together, our results indicate that Ahi1 mediates feeding behavior by interacting with 5-HT$_{2C}$R to modulate the serotonin signaling pathway.

Obesity and its associated ailments such as diabetes have become a worldwide epidemic carrying with them a heavy toll of morbidity and mortality. Over the past decades, it has become evident that neural circuits in the central nervous system play a direct and crucial role in controlling feeding and energy homeostasis (1, 2). Disruptions in the mechanisms of central nervous system energy sensing are able to alter the standard homeostatic responses and are factors that contribute to the pathophysiology of obesity and diabetes. The brain serotonin system has long been implicated in the neural regulation of food intake and energy metabolism, as highlighted by the clinical use of serotonin releasers and reuptake inhibitors as appetite suppressant and weight loss medication (3–5). Depletion of central serotonin using selective neurotoxins has been shown to result in hyperphagia and obesity, whereas the release of serotonin and the inhibition of reuptake by D-fenfluramine potently reduce feeding and body weight (6). More recently, several lines of evidence show that serotonin receptor agonists can significantly improve glucose tolerance and reduce plasma insulin in mouse models of obesity and type 2 diabetes (7–9).

Numerous serotonin receptor subtypes have been identified in which serotonin receptor 2C (5-HT$_{2C}$R)[4] is recognized specifically as a mediator of serotonin-induced appetite and glucose regulation (10–13). During the past few years, both pharmacological and genetic evidence has indicated that neuropeptide Y (NPY) and melanocortin systems are the necessary mechanisms by which 5-HT$_{2C}$R agonists reduce appetite and improve diabetic conditions (14–16). Although significant progress has been made in the study of serotonin-mediated regulation of energy metabolism, we are still far from understanding the whole picture. One of the more intriguing aspects of this area that has remained mysterious is the importance of cellular and molecular interactions that regulate energy homeostasis centrally.

Abelson helper integration site 1 (Ahi1) was initially identified as a common helper provirus integration site for murine leukemia and lymphomas (17). A number of groups have identified *Ahi1* mutations as a frequent cause of disease in patients with specific forms of Joubert syndrome, an autosomal recessive neurodevelopmental disorder, and its related disorders (JSRD) (18–20). The normal neural function of Ahi1, however, remains poorly defined. Both protein and mRNA studies have shown that Ahi1 is distributed in several brain areas implicated in feeding and metabolic regulation such as the hypothalamic

paraventricular nucleus, the supraoptic nucleus, the arcuate nucleus (ARC), the lateral hypothalamic area, and the nucleus tractus solitarius in the brain stem (21–23). Genetic studies also indicate that Ahi1 may be related to energy metabolism. One group has reported a significant association between variants in the *Ahi1* gene and type 2 diabetes in a Dutch population (24). In addition, single nucleotide polymorphism association studies identified two novel Ahi1 genetic variants linked with fasting blood glucose levels in Mexican American subjects (25). Recent studies (26, 27) also show that brain Ahi1 may play an important role in the regulation of feeding behavior.

We noticed that Ahi1 and 5-HT$_{2C}$R have similar distribution in the hypothalamus. This prompted us to investigate the relationship between Ahi1 and 5-HT$_{2C}$R and their probable roles in feeding control. The findings in the present study provide evidence that Ahi1 interacts with 5-HT$_{2C}$R to mediate feeding behavior. Our study reveals the normal neural function of Ahi1 in feeding control and offers insight into the understanding of how hypothalamic key molecules regulate the feeding behavior.

MATERIALS AND METHODS

Animals—Male C57BL/6J mice, 6–10 weeks old, were purchased from Southern Medical University, Guangdong Province, China. The animals were housed in a temperature- and humidity-controlled environment with a 12 h/12 h light/dark cycle with access to food and water *ad libitum*. Animals were acclimatized to laboratory conditions for a week before all tests. Animal care and all procedures for animal experiments conformed to the guidelines of the Animal Care and Use Committee of Guangzhou Biomedical and Health Institute, Chinese Academy of Sciences.

Immunostaining—The antibody against Ahi1 is described in our previous study (23). For immunofluorescent staining, sections of brain tissue and coverslips plated with hypothalamic neurons or HEK293 cells were blocked with 5% bovine serum albumin (BSA) in 0.02 M PBS at room temperature for 1 h and followed by incubating with rabbit anti-Ahi1 antibody (1:300) and goat anti-5-HT$_{2C}$R (1:50, Santa Cruz Biotechnology) at 4 °C overnight. Then the sections were incubated successively with Alexa Fluor 488-conjugated anti-goat secondary antibody and Alexa Fluor 594-conjugated anti-rabbit secondary antibody (both from Invitrogen) at room temperature for 30 min. Tissue sections and coverslips were mounted onto glass slides. Labeled samples were imaged using a ×100 objective Leica SP2 confocal microscope.

Immunoprecipitation—Lysates from mouse hypothalami or from co-transfected HEK293 cells were extracted using lysis buffer (50 mM Tris-Cl, pH 8.0, 150 mM NaCl, 1 mM EDTA, 1 mM EGTA, 1% Triton X-100, and protease inhibitor mixture) and centrifuged at 12,000 × g at 4 °C for 15 min. 500 μl of supernatant (adjusted to 1 mg/ml) was first clarified by incubation with 40 μl of 50% protein A-Sepharose beads (Sigma) at 4 °C for 1 h to reduce nonspecific binding. After pelleting the beads, the supernatant was then incubated with antibody to mouse Ahi1 (1:50), anti-hemagglutinin (HA) monoclonal antibody (Sigma, clone HA-7, diluted 1:4000), anti-GFP polyclonal antibody (Abcam, ab290, diluted 1:1000), or immunoglobulin G as control overnight at 4 °C followed by brief centrifugation. The

immunoprecipitates were washed three times with low detergent buffer (50 mM Tris-Cl, pH 8.0, 150 mM NaCl, 1 mM EDTA, 1 mM EGTA, and 0.2% Tween 20) and subjected to Western blotting.

Purification Membrane Fraction and Western Blot—A total of 15–20 mg of whole hypothalami from fasted mice or Ahi1 knockdown mice were adequately blended in 1 ml of pre-cold membrane purification buffer (MPB: 250 mM sucrose, 30 mM KCl, 20 mM Tris-Cl, pH 7.2, 0.2 mM DTT, 1 mM EDTA, 1 mM EGTA, 0.3% Triton X-114, and protease inhibitor mixture) on ice. The suspensions were ultracentrifuged at 59,000 × g at 4 °C for 15 min, and then the pellets (P1) were re-extracted as mentioned above in 1 ml of MPB with 0.8% Triton X-114. After a 30-min incubation on ice, the soluble materials were removed by ultracentrifugation (as above). The pellets (P2, purified membrane fraction) were washed twice with MPB and finally resuspended in MPB.

Hypothalami were mechanically homogenized and sonicated in homogenization buffer on ice. 20 μg of tissue protein was size-fractionated using 10% SDS-PAGE and electrotransferred onto nitrocellulose membranes. Cell lysates (50 μg) from treated N18TG2 cells were also subjected to SDS-PAGE and blotted. After blotting with the antibodies, anti-mouse Ahi1 or anti-5-HT$_{2C}$R and anti-γ-tubulin (Sigma), anti-β-actin (ACTB, GenScript), and anti-LAMP1 detection was performed using an enhanced chemiluminescent kit (Pierce) according to the manufacturer's instructions. Quantitations of gray density were performed using ImageQuant 5.2 software.

Quantitative RT-PCR—Total RNA was isolated from tissue samples or cell samples using TRIzol reagent (Ambion). cDNA was synthesized by using Moloney murine leukemia virus (MMLV) reverse transcriptase (Fermentas). Primers for mouse Ahi1 (forward primer, 5′-GAC AGG AGA ACA AGT GGC AAT G-3′; reverse primer, 5′-ATC AGT GGT CAG CAC GAA CGA-3′), mouse NPY (forward primer, 5′-TAC TAC TCC GCT CTG CGA CAC-3′; reverse primer, 5′-CCA CAT GGA AGG GTC TTC AAG-3′), mouse proopiomelanocortin (POMC) (forward primer, 5′-CGA GCG GCC ATT AGG CTT-3′; reverse primer, 5′-CTT GTC CTT GGG CGG GTT-3′), and reference gene GAPDH (forward primer, 5′-CTG CAC CAC CAA CTG CTT AGC-3′; reverse primer, 5′-GGA AGG CCA TGC CAG TGA-3′) were optimized to an equal annealing temperature of 60 °C. Expression of Ahi1, NPY, POMC, and GAPDH was determined by real-time PCR using SYBR® Premix Ex Taq (Takara) on an MJ four-color real-time PCR system (Bio-Rad) according to the manufacturer's instructions. The expression ratio of target genes among the experimental groups was calculated and statistically analyzed as reported previously (28, 29).

RNA Interference—For the knockdown of Ahi1, C57BL/6J mice (8-week-old males) were injected bilaterally with recombinant adenovirus vector encoding Ahi1-specific siRNA (AdsiAhi1) or scramble-siRNA (Ad-scRNA) as control. A total of 1×10^{11} plaque-forming units in 1 μl of PBS were injected bilaterally intrahypothalamus at the stereotaxic positions (anteroposterior −1.1 mm, mediolateral −0.5 mm, dorsalventral −5.5 mm; anteroposterior −1.1 mm, mediolateral +0.5 mm, dorsalventral −5.5 mm). The adenoviral vector also inde-

pendently expresses green fluorescent protein (GFP), which enabled us to trace the vector. Injection at the above coordinates allowed the adenovirus to mainly infect the ventromedial hypothalamus, ARC, dorsomedial hypothalamus, and other nuclei in the hypothalamus (Fig. 4*A*). The mice were single-housed in regular plastic cages before and after the surgical procedure. Food intake and body weight were recorded daily for 4 weeks. After a period of 3–5 days post-surgical recovery, the mice were tested for glucose tolerance tests and insulin tolerance tests performed as described previously (30). Glycemia was assessed using a blood glucose test meter.

Cell Culture, Infection, Transfection, and Drug Treatment—Co-localization of Ahi1 and 5-HT$_{2C}$R was observed on the networks of cultured mice hypothalamic neurons. The details of culture preparations have been described previously (31). In brief, hypothalamic tissue was dissected from newborn mice. Hypothalamic neural cells were planted on poly-D-lysine-coated coverslips at a density of ~2000 cells/cm^2. Cultures were kept in Neurobasal medium supplemented with 2% B27 and 2 mM L-glutamine (all from Invitrogen) for 14 days *in vitro*.

N18TG2 cells, the mouse neuroblastoma cell line with endogenous Ahi1 expression, were grown in high glucose Dulbecco's modified Eagle's medium (DMEM, Invitrogen) supplemented with 10% fetal bovine serum (PAA Laboratories), 1 mM non-essential amino acids (Invitrogen), 2 mM L-glutamine (Invitrogen), 100 units/ml penicillin, and 100 μg/ml streptomycin (Invitrogen). DNA constructs for expression of Ahi1 cDNA plasmids encoding full-length mouse Ahi1-(1–1047) were generated as in a previous study (32). We used PCR to generate C-terminally truncated mouse Ahi1-(1–820). These Ahi1 cDNAs were sequenced and cloned to the PRK vector that links the influenza HA epitope on the upstream of the Ahi1 coding region. For transfection of foreign DNAs into N18TG2, plasmid-polyethylenimine (Polysciences, Inc.) complexes incubated with cultures for 1 h. After 36 h of transfection, N18TG2 cells were stimulated under 5 μM *meta*-chlorophenylpiperazine (mCPP; Sigma) with or without 100 μM chloroquine (Chlq; Sigma) for the indicated time and then immediately collected for the following quantitative assays. For virus infection, the cells were infected by Ad-siAhi1 (1 × 10^7 plaque-forming units/ml medium) for 8 h and sampled at 24 h post-infection.

HEK293 cells were cultured in DMEM containing 10% fetal bovine serum, 1 mM sodium pyruvate, 2 mM L-glutamine, 100 units/ml penicillin, and 100 μg/ml streptomycin. When 50% confluence had been achieved, the HEK293 cells were co-transfected with constructs encoding DsRed-tagged Ahi1 and GFP-tagged 5-HT$_{2C}$R as described above.

Immunofluorescence Labeling with LAMP1 and Quantification of the Co-localization of 5-HT$_{2C}$R and LAMP1—N18TG2 cells, co-transfected with PRK-mAhi1-DsRed/PRK-DsRed and GFP-5-HT$_{2C}$R, were washed once, fixed for 10 min at −20 °C in 50% (v/v) acetone/methanol, and air-dried. Cells were blocked by incubating them for 1 h in 5% BSA and then with anti-LAMP1 primary antibody (4 μg/ml, Abcam) at 4 °C for 24 h. Then coverslips were washed several times and incubated with Cy5-labeled anti-mouse IgG for 45 min at room temperature. After DAPI staining, four-color slides were visualized with a Leica SP2 confocal scanning microscope set up as follows: 403

nm laser (25% of power) window, 410–483 nm; 488 laser (25% of power) window, 493–538 nm; 543 nm laser (90% of power) window, 548–628 nm; and 633 nm laser (25% of power), window 638–700 nm. Images were collected using the microscope in sequential mode with a frame average and a format of 1024 × 1024 pixels and were analyzed using NIH ImageJ 1.40g software. For statistical analyses, images for all conditions were analyzed using identical acquisition parameters, and untreated and treated cells from the same culture preparation were always compared with one another. The images were also collected blind to experimental condition. The total thresholded area of fluorescently labeled overlay regions was automatically measured and divided by the total cell area, which was determined by setting a lower threshold level to measure the background fluorescence produced by the fixed cells. For each experiment, the fluorescence of all cells was normalized by dividing the average fluorescence of the untreated control cells. All cells that expressed 5-HT$_{2C}$R with less than the average at 30% were excluded from analysis because of the variation in transfection efficiency.

Statistics—GraphPad Prism was utilized for data analysis. Data are presented as mean ± S.E. of at least three independent experiments. Statistical analyses were carried out by one-way analysis of variance followed by Tukey's post hoc test, and $p <$ 0.05 was considered statistically significant.

RESULTS

Co-localization and Interaction between Hypothalamic Ahi1 and 5-HT$_{2C}$R—First, we cultured hypothalamic neurons *in vitro*. In double-labeled immunofluorescence staining assays of cultured hypothalamic neurons, Ahi1 was observed to co-localize significantly with 5-HT$_{2C}$R (Fig. 1*A*, *top* and *middle rows*). Staining of mouse brain sections also revealed an extensive overlap of the two proteins in hypothalamus nucleus such as ARC (Fig. 1*A*, *bottom row*). A co-immunoprecipitation study was performed in mice hypothalamus homogenates. As shown in Fig. 1*B*, 5-HT$_{2C}$R selectively bound to endogenous Ahi1, whereas no signal was detected in immunoprecipitates from non-immune rabbit serum control. To confirm this physical interaction, we subsequently expressed them in transfected HEK293 cells; GFP-5-HT$_{2C}$R showed an extensive distribution throughout the plasma membrane and cytoplasm of the cell, whereas Ahi1 showed a unique distribution pattern characterized as dot-like structures. Co-expression of 5-HT$_{2C}$R and Ahi1 displayed apparent co-localization in punctate aggregates in the cytoplasm of HEK293 cells (supplemental Fig. 1*A*). Their interaction was further demonstrated by co-immunoprecipitation using anti-Ahi1 antibody (supplemental Fig. 1*B*). Then, we constructed the C terminal-truncated Ahi1. In the immunofluorescence experiments, we found that the co-localization of Ahi1 and 5-HT$_{2C}$R was lost in the cells transfected with C terminal-truncated Ahi1 (Fig. 1*D*). Similarly the combination of Ahi1 and 5-HT$_{2C}$R was abolished in the C terminal-truncated Ahi1 (Fig. 1*E*). These data indicate that the C terminus of Ahi1 is the region where it interacts with 5-HT$_{2C}$R.

Ahi1 Promotes Lysosomal Degradation of 5-HT$_{2C}$R—Given the WD40 repeat domains and the SH3 domain found in the Ahi1 protein (32), we hypothesized that Ahi1 may play a role in neurotransmitter receptor trafficking as an adaptor between
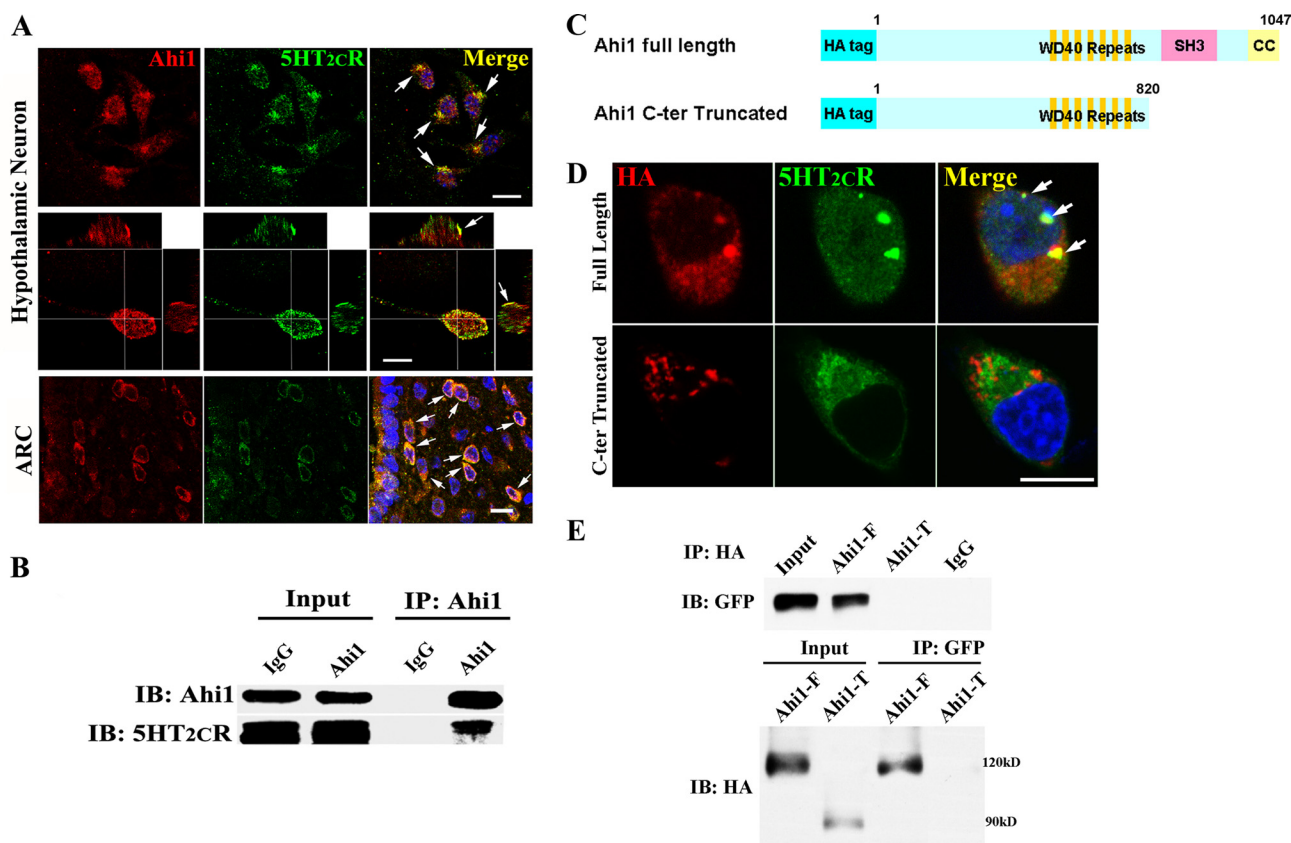
FIGURE 1. **Hypothalamic Ahi1 co-localized and interacted with 5-HT$_{2C}$R.** *A*, immunofluorescence analysis of the co-localization between Ahi1 and 5-HT$_{2C}$R in cultured hypothalamic neurons and in a hypothalamus ARC sections. Ahi1 co-localized significantly with 5-HT$_{2C}$R in the soma of hypothalamic neurons (*top row*, two-dimensional photo; *middle row*, three-dimensional photo; *arrows* indicate co-localization of Ahi1 and 5-HT$_{2C}$R) and the hypothalamus nucleus such as ARC (*bottom row*). *B*, 5-HT$_{2C}$R was co-precipitated by the Ahi1 antibody in the hypothalamus of mice. *C*, schematic of full-length Ahi1 and C terminus truncated Ahi1. *D*, full-length or truncated Ahi1 was co-transfected with 5-HT$_{2C}$R into HEK293 cells, and then immunofluorescence was performed. Note that in the cells transfected with truncated Ahi1, co-localization of Ahi1 and 5-HT$_{2C}$R was lost. *E*, co-immunoprecipitation showed that the combination of Ahi1 and 5-HT$_{2C}$R was abolished in C terminal-truncated Ahi1. *Scale bar*: 20 μm. *C-ter*, C terminus; *Ahi1-F*, Ahi1 full-length; *Ahi1-T*, truncated Ahi1; *IP*, immunoprecipitation; *IB*, immunoblotting.

cytoskeleton and membrane protein. It has been reported that Ahi1 participates in the process of intracellular vesicle trafficking and is co-localized with microtubules and the microtubule-organizing center (33, 34). We postulated that Ahi1 could participate in 5-HT$_{2C}$R vesicles sorting to degradation after endocytosis. To test this hypothesis, we treated cells with mCPP, an agonist of 5-HT$_{2C}$R (13). As shown in Fig. 2*A*, the 5-HT$_{2C}$R decreased in a time-dependent way in the cells transfected with full-length Ahi1, whereas in the cells transfected with truncated Ahi1 this decrease was inhibited. Then we addressed the pathway of 5-HT$_{2C}$R degradation. We first investigated the possible involvement of the lysosomal pathway by treatment with Chlq, a lysosomal enzyme inhibitor. Analysis by Western blot revealed that treatment with Chlq increased the level of 5-HT$_{2C}$R in mCPP treated N18TG2 cells (Fig. 2*B*, *lane 3 versus lane 2*), thereby indicating that the lysosomal pathway mediates internalized 5-HT$_{2C}$R degradation. To address the possible function of Ahi1 in lysosomal sorting, we investigated whether the expression of Ahi1 affects the degradation of internalized serotonin receptors. When we co-transfected with a RFP-Ahi1 vector, the degradation of activated 5-HT$_{2C}$R was significantly increased as compared with that of an empty vector (Fig. 2*B*, *lane 5 versus lane 2*), and this increased 5-HT$_{2C}$R degradation could be blocked by adding Chlq to the cells (Fig.

2*B*, *lane 6*). As shown in supplemental Fig. 2, the addition of lactacystin (a proteasome inhibitor) could not block the degradation of 5-HT$_{2C}$R, which indicates that the proteasome pathway is not involved in the 5-HT$_{2C}$R degradation. In the cells expressing GFP-5-HT$_{2C}$R alone, the receptor was distributed throughout the plasma membrane as well as the cytoplasm when visualized under the fluorescence microscope (Fig. 2*C*, *bottom row*). Co-expression of Ahi1 dramatically changed the distribution pattern of 5-HT$_{2C}$R as expected, and strong 5-HT$_{2C}$R signals were overlapped with LAMP1 (as lysosome marker) positive dots, where 5-HT$_{2C}$R co-localized with Ahi1 (Fig. 2*C*, *top row*). Quantification of 5-HT$_{2C}$R and LAMP1 co-localization (Fig. 2*D*) showed significant overlapping regions between the 5-HT$_{2C}$R and LAMP1-labeled pixels when Ahi1 was expressed (563.49% of mCPP-untreated cells, a total of 34 cells were quantified). However, the value was much lower when Ahi1 was absent (109.90% of mCPP-untreated cells, a total of 32 cells were quantified). Taken together, these results strongly support the idea that Ahi1 interacts with 5-HT$_{2C}$R and enhances the trafficking of internalized 5-HT$_{2C}$R to lysosomes, thereby promoting its degradation.

Fasting Alters Expression of Hypothalamic Ahi1 and 5-HT$_{2C}$R —We then examined the role of hypothalamic Ahi1 and 5-HT$_{2C}$R in the regulation of feeding behavior. As shown in
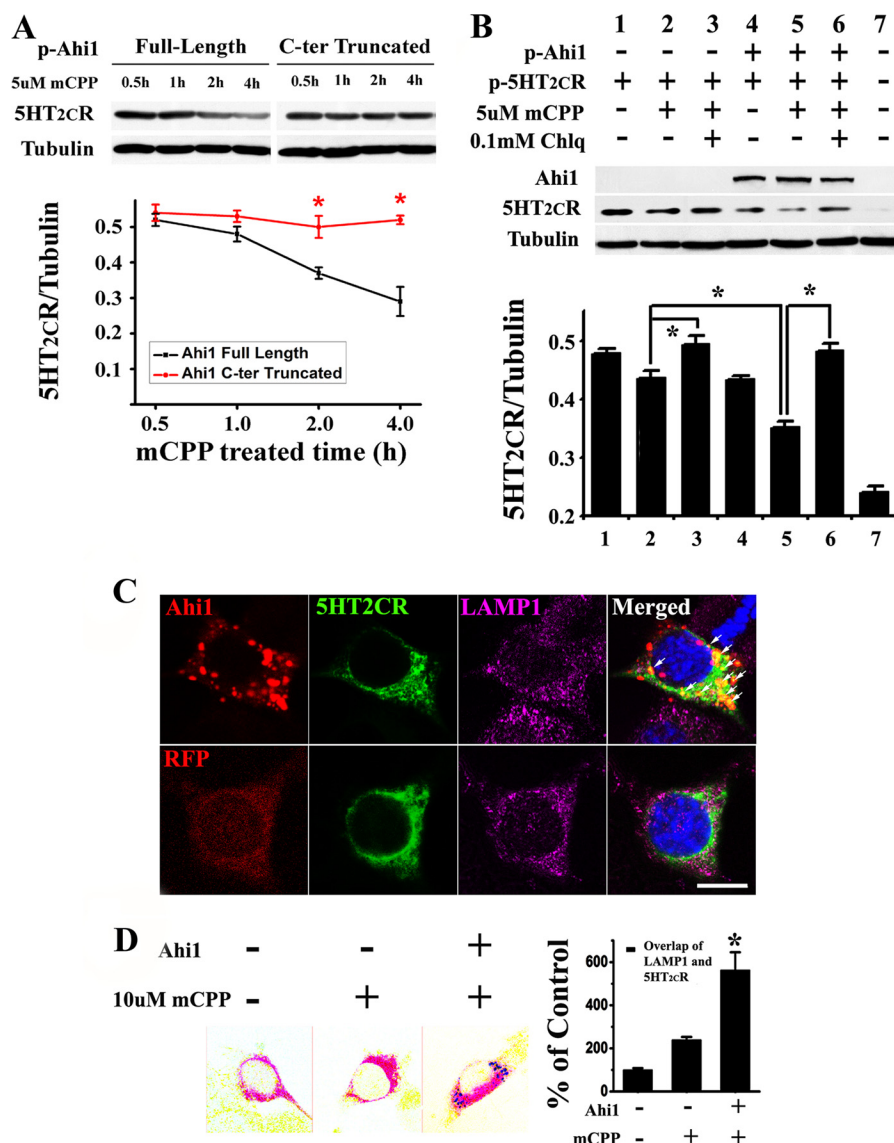
FIGURE 2. **Ahi1 promoted the degradation of 5-HT$_{2C}$R through the lysosomal pathway.** *A*, full-length or truncated Ahi1 was co-transfected with 5-HT$_{2C}$R into N18TG2 cells, and then immunoblotting was performed. In the cells transfected with full-length Ahi1, 5-HT$_{2C}$R decreased in a time-dependent way after mCPP treatment, whereas in the cells transfected with truncated Ahi1 this decrease was inhibited. *B*, co-expression of 5HT$_{2C}$R with Ahi1 in N18TG2 cells led to increased degradation of mCPP-activated 5-HT$_{2C}$R compared with the expression of 5-HT$_{2C}$R alone (*lane 5* compared with *lane 2*), which could be blocked under the application of Chlq (*lane 6*). *C*, 5-HT$_{2C}$R located in the lysosomes was increased in the presence of Ahi1. In cells expressing GFP-5-HT$_{2C}$R and RFP-Ahi1, the 5-HT$_{2C}$R mainly overlapped with the lysosomes (LAMP1 as marker) and co-localized with Ahi1 (*top row*, indicated by *arrows*). In the absence of Ahi1, 5-HT$_{2C}$R is distributed throughout the plasma membrane as well as the cytoplasm (*bottom row*). *D*, quantifying the co-localization of 5-HT$_{2C}$R with the lysosomes in N18TG2 cells by calculating the area containing 5-HT$_{2C}$R and lysosome-labeled pixels with or without Ahi1. *Scale bar*: 10 μm. Data are expressed as mean $\pm$ S.E. *, statistically different from control group. *C-ter*, C terminus; *p-Ahi1*, plasmid-Ahi1; *p-5HT$_{2C}$R*, plasmid-5HT$_{2C}$R; *LAMP1*, lysosome-associated membrane protein 1; *RFP*, red fluorescent protein.

Fig. 3*A*, hypothalamic Ahi1 protein was significantly increased after a fasting period of 24 or 48 h. Similarly, the transcription of Ahi1 mRNA was significantly up-regulated (Fig. 3*B*). To investigated the involvement of 5-HT$_{2C}$R in this process, we isolated the member fraction of hypothalamus lysates and assessed 5-HT$_{2C}$R located on the neuronal membrane under the condition of fasting. As shown in Fig. 3*C*, the down-regulation of membrane 5-HT$_{2C}$R levels was concomitant with the up-regulation of Ahi1 in the time course study. To further confirm the correlation between 5-HT$_{2C}$R and Ahi1, We employed pharmacological modulators of 5-HT$_{2C}$R (mCPP and olanzapine). First, we pretreated (intraperitoneally) fasted mice with mCPP, an agonist of 5-HT$_{2C}$R. The up-regulation of hypothalamic

Ahi1 in fasted mice was significantly inhibited by mCPP pretreatment (Fig. 3*D*). Then, we used olanzapine, an antagonist of 5-HT$_{2C}$R (35). The expression of Ahi1 protein in the N18TG2 cell line, as shown in supplemental Fig. 3*A*, was increased by 70% after 72 h of exposure to olanzapine. Similarly, as compared with the control group, 4 weeks of treatment with olanzapine significantly increased the levels of Ahi1 expression in the mice hypothalami (supplemental Fig. 3*B*). These data suggest that 5-HT$_{2C}$R is a necessary component of the Ahi1-dependent signaling pathway that controls feeding behavior.

Knockdown of Hypothalamic Ahi1 Suppresses Food Intake— To further establish a role for endogenous Ahi1 in feeding, we used RNA interference (RNAi) to suppress the expression of
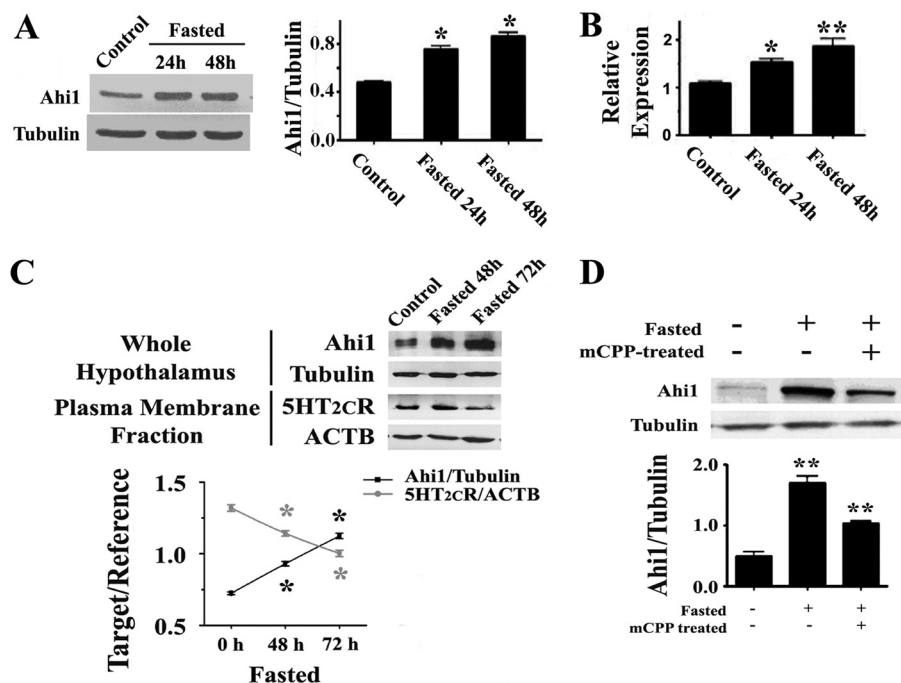
FIGURE 3. **The expression of hypothalamic Ahi1 and 5-HT$_{2C}$R was changed by fasting.** *A*, Western blot showed that the protein levels of Ahi1 were significantly increased after fasting mice for 24 or 48 h. *B*, real-time PCR demonstrated that the transcription of hypothalamic Ahi1 mRNA was also stimulated by fasting. *C*, 5-HT$_{2C}$R located on the neuronal membrane under the conditions of fasting. When the expression of hypothalamic Ahi1 was up-regulated by fasting, the level of 5-HT$_{2C}$R on the membrane of hypothalamic neurons was significantly reduced. *D*, up-regulation of hypothalamic Ahi1 induced by fasting was significantly inhibited by mCPP pretreatment. Data are expressed as mean ± S.E. *, statistically different from control group. *ACTB*, β-actin.

Ahi1 in the hypothalamus. We generated a mouse Ahi1-specific siRNA that effectively inhibited the expression of endogenous Ahi1 in N18TG2 cells (supplemental Fig. 4). This siRNA was expressed from an adenoviral vector that also independently expressed GFP. Thus, cells labeled with GFP should also express Ahi1-specific siRNA. An adenoviral vector expressing scramble-siRNA (Ad-scRNA) served as a control. As shown in Fig. 4*A*, a high level of expression of GFP-fused Ad-siAhi1 4 days post-injection (dpi) was observed on stereotactic coronal sections. Immunohistochemistry (Fig. 4*B*) and Western blot (Fig. 4*C*) showed that Ad-siRNA produced a significant knockdown of Ahi1 protein in the hypothalamus. After surgery, the animals were housed individually. Food intake and body weight were measured daily for 4 weeks. As shown in Fig. 4*D*, food intake in the Ad-siAhi1 mice and the control mice was minimal immediately following surgery. After 24 h, both groups started to increase their food intake. However, the Ad-siAhi1 mice consumed significantly less food compared with the control mice, and thus the difference remained relatively constant throughout the first 2 weeks. The food intake of Ad-siAhi1 mice gradually returned to a normal level after 2 weeks, possibly because of the invalidating of Ad-siRNA over time. Correspondingly, body weight also showed a dramatic decrease in both groups in the beginning. Subsequently, body weight gradually increased in the control mice, but it decreased until the fifth day in the Ad-siAhi1 mice. The average body weight of the Ad-siAhi1 mice was significantly lower than the control group throughout the testing period (Fig. 4*E*). We further investigated the effects of hypothalamic Ahi1 knockdown on glucose metabolism. Mice on 5, 10, and 15 dpi underwent glucose tolerance tests and insulin tolerance tests separately. The glucose toler-

ance tests revealed that on 5 and 10 dpi, but not on 15 dpi, Ad-siAhi1-treated mice exhibited a significant improvement of glucose tolerance as compared with control mice (Fig. 4*F*). In insulin tolerance tests, Ad-siAhi1 mice exhibited an apparent improvement in insulin sensitivity (Fig. 4*G*). The Ad-siAhi1 mice became significantly more hypoglycemic at 30 min on 5 dpi and at 30 and 60 min on 10 dpi after insulin injection than did the control mice. We also assessed 5-HT$_{2C}$R located on the neuronal membrane under the condition of artificial Ahi1 knockdown (supplemental Fig. 5). When Ahi1 expression was knocked down by RNAi (at 7 or 14 days post-surgery), membrane 5-HT$_{2C}$R was significantly increased, after which a regression followed that was due to Ahi1 expression recovery.

Ahi1 Regulates Expression of NPY and POMC—Lastly, we explored the downstream targets of the hypothalamic Ahi1 signaling pathway in feeding control. Previous reports (15, 16, 36) have revealed that serotonin receptors activation inhibits the expression of orexigenic NPY and yet stimulates the expression of anorexigenic POMC in the hypothalamus. Because Ahi1 inhibits the activity of 5-HT$_{2C}$R, we hypothesized that Ahi1 may also regulate the expression balance of NPY and POMC. The abundance of NPY and POMC mRNA was measured using real-time quantitative PCR. Notably, knockdown expression of Ahi1 led to a decrease in the mRNA levels of NPY and an increased expression of POMC in neuronal cell line N18TG2. In contrast, overexpression of Ahi1 resulted in higher NPY expression and lower POMC production (Fig. 5*A*). Moreover, Ad-siAhi1 intrahypothalamic injection reduced the mRNA level of NPY by 35% and increased the mRNA level of POMC by 49% in the mice hypothalami on day 3 post-injection. Similar changes in the level of POMC and NPY by Ad-siAhi1 treatment
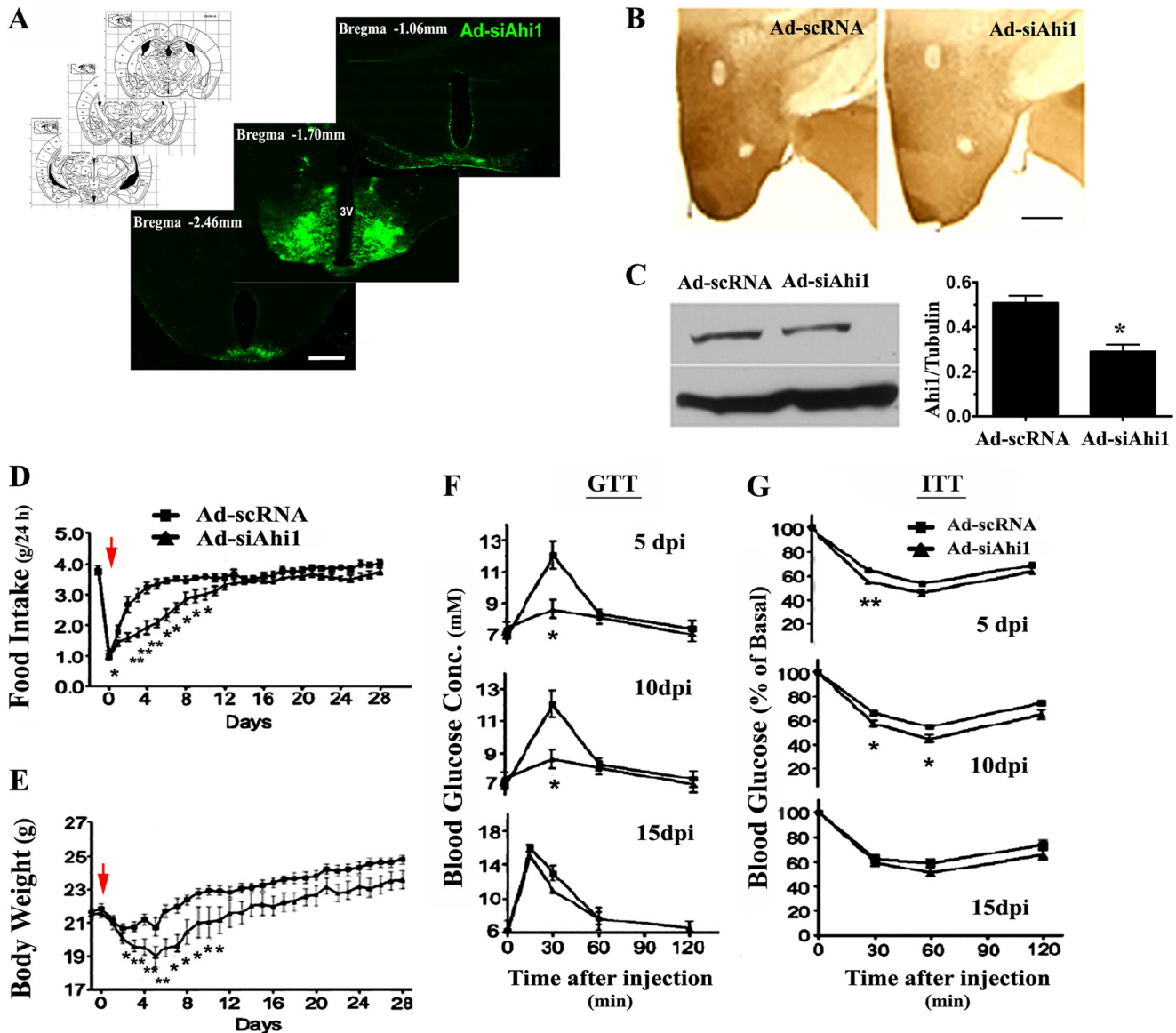
FIGURE 4. **Knockdown of hypothalamic Ahi1 led to a decrease in food intake and body weight and an improvement in glucose tolerance and insulin sensitivity.** *A*, Ad-siAhi1 (GFP labeling) was expressed in the majority of the hypothalamus, including dorsomedial hypothalamus, ventromedial hypothalamus, and ARC. The fluorescent microscopic image shows the expression of adenoviral vectors with stereotaxic position. Ad-siAhi1 or Ad-scRNA (as control) vector was delivered bilaterally into the mice hypothalamus. Immunohistochemistry (*B*) and Western blot (*C*) showed that Ad-siRNA produced a significant knockdown of Ahi1 protein in the hypothalamus. Animals were fed with a regular chow diet for 4 weeks post-injection. Accumulative food intake (*D*) and body weight (*E*) during the 4-week post-injection time were measured (*red arrows*, indicate injection day). *F*, a glucose tolerance test (*GTT*) was performed by measuring blood glucose concentration at 30, 60, 90, and 120 min after intraperitoneal injection of glucose in Ad-siAhi1 mice and Ad-scRNA control mice on days 5, 10, and 15. *G*, an insulin tolerance test (*ITT*) was performed by measuring blood glucose abundance in Ad-siAhi1 mice and Ad-scRNA control mice at the indicated times after intraperitoneal injection of insulin. *Scale bar*: 200 μm in *A*; 100 μm in *B*. Data are expressed as mean $\pm$ S.E. *, statistically different from Ad-scRNA group. *Ad-siAhi1*, adenoviral vector with Ahi1-specific siRNA; *Ad-scRNA*, adenoviral vector with scramble-siRNA.

were also found on day 9 post-injection (Fig. 5*B*). These changes in feeding-related neuropeptides are consistent with decreased appetite as illustrated in Fig. 4*D*.

DISCUSSION

Although much progress has been made in understanding how neural circuits control feeding behavior and energy metabolism, we are far from getting the whole picture. Many other important cellular and molecular interactions within the circuits remain unknown. Our study indicates that hypothalamic Ahi1 could be one of the important interaction molecules within the circuits. Its high expression in the central nervous

system and its structural characteristics make Ahi1 an ideal candidate for signal transduction in the central nervous system. Ahi1 contains several distinct protein domains, including six WD40 repeats, one SH3 domain, potential SH3 binding sites, and an N-terminal coiled-coiled domain (32). WD40 domains have been found in proteins involved in a variety of functions including signal transduction, RNA processing, transcriptional regulation, cytoskeleton assembly, vesicle trafficking, and cell division (37). Similarly, SH3 domains are a common feature of signaling molecules involved in numerous pathways (38, 39). Multiple lines of evidence have shown Ahi1 as a key regulator of neuronal development. *Ahi1* mutation not only causes defects

A

B

C

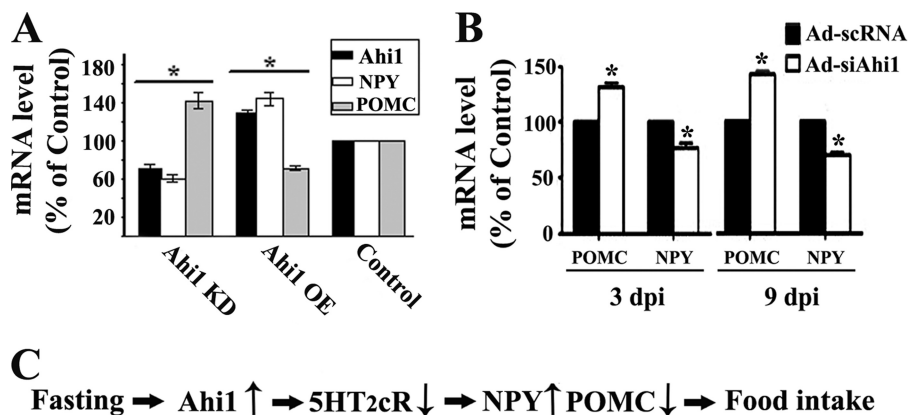Fasting ➡ Ahi1↑ ➡ 5HT2cR↓ ➡ NPY↑ POMC↓ ➡ Food intake

FIGURE 5. **Ahi1 modulated the expression of NPY and POMC.** *A*, Ahi1 regulated the transcription of POMC and NPY in N18TG2 cells. Quantitative RT-PCR indicated that down-regulation of Ahi1 by siRNA decreased NPY and increased POMC expression, whereas overexpression of Ahi1 resulted in higher NPY expression and lower POMC production. *B*, knockdown of Ahi1 in mice hypothalami led to an increase in POMC mRNA and a decrease in NPY mRNA on days 3 and 9 post-injection. *C*, proposed model of hypothalamic Ahi1 in feeding control. Data are expressed as mean ± S.E. *, statistically different from control group. *KD*, knockdown; *OE*, overexpression.

in intracellular trafficking (40) but also leads to abnormal development of neuronal interactions and networks. The dysfunction of Ahi1 causes developmental disorders. Abnormal cerebellar and cortical development as well as lack of axonal decussation is caused by *Ahi1* mutation in Joubert syndrome and related disorders (18, 22). Moreover, our previous study has proven that dysfunctional interaction of Hap1-Ahi1 causes defects in axonal guidance and alters brain connections in the postnatal brainstem and cerebellum (23). The present study showed that under normal conditions hypothalamic Ahi1 interacts with 5-HT$_{2C}$R to regulate food intake. The 5-hydroxytryptamine (serotonin) system has long been associated with food intake and body weight regulation. A variety of studies have demonstrated that hypothalamic NPY and POMC are important intermediaries in the serotonin system-induced feeding response (15, 16, 41–43). Serotonin receptor activation inhibits the expression of orexigenic NPY and stimulates the expression of anorexigenic POMC in the hypothalamus (15, 16, 36). Two sets of neurons, with opposite effects on feeding, have been identified in the hypothalamic arcuate nucleus: the POMC and NPY neurons. The neurons that express POMC are anorexigenic, due to the release of the cleavage products of POMC precursor (α- and β-melanocyte-stimulating hormones (α-/β-MSH) (44, 45)), which in turn reduce food intake and body weight as well as increase energy expenditure in animals and humans (46–48) by acting on melanocortin receptor subtypes 3 and 4 (MC3R and MC4R) (49). In contrast, the neurons containing NPY are orexigenic (50). NPY potently stimulates food intake and reduces energy expenditure (51). In this study, we have demonstrated the important role that Ahi1 plays in the endocytic sorting of 5-HT$_{2C}$R. After endocytosis, Ahi1 facilitates the trafficking of 5-HT$_{2C}$R to lysosomal compartments. As such, the anorectic effect of the 5-HT$_{2C}$R pathway is counteracted by Ahi1 through the transportation of the receptors to the lysosomes for degradation. A previous study has shown that 5-HT$_{2C}$R is expressed in POMC-containing neurons (52), and we speculate that Ahi1 inhibits POMC expression by trafficking 5-HT$_{2C}$R to the lysosome for degradation. Considering that the NPY-containing neurons are not co-expressed with 5-HT$_{2C}$R, we hypothesize that the effect of Ahi1 on stimulating NPY

expression is most likely mediated indirectly by other molecular pathways. On the other hand, blockade of Ahi1-dependant lysosomal sorting will increase the functional expression of 5-HT$_{2C}$R (supplemental Fig. 5). Knockdown of Ahi1 expression leads to less 5-HT$_{2C}$R trafficking into lysosomes, consequently resulting in the stimulation of POMC expression and the inhibition of NPY expression (Fig. 5*B*) that subsequently reduce food intake (Fig. 4*D*) and decrease body weight (Fig. 4*E*).

Interestingly, we observed an increased level of Ahi1 expression in olanzapine-treated mice (supplemental Fig. 3). There is a growing concern about the increased risk of diabetes in patients with schizophrenia, where normal health risks are elevated by the obesogenic and diabetogenic side effects of antipsychotics (53–55). It has been found that the risk is greater with the atypical antipsychotics such as olanzapine, which has serotonin receptor antagonist properties (56). It has been demonstrated that olanzapine is associated with significant antipsychotic-induced weight gain (57) and impaired glucose effectiveness (58). However, the mechanisms responsible for the diabetes mellitus associated with some antipsychotics are still not fully understood. It has been proposed that the specific binding profile of different antipsychotic agents may help explain the occurrence of particular side effects associated with each drug (59). Among the multiple receptor binding profiles of atypical antipsychotics, 5-HT$_{2C}$R has been implicated as mediating an orexigenic effect and diabetogenic side effect. The agonists of 5-HT$_{2C}$R, such as fenfluramine and mCPP, have been shown to be anorexigenic (60, 61). There is a correlation between the drug affinity for 5-HT$_{2C}$R and the morbidity rate of type 2 diabetes mellitus (62). We speculate that Ahi1 may be involved in the metabolic side effects of atypical antipsychotics. The use of olanzapine will result in increased hypothalamic Ahi1 expression. In the short term, Ahi1 will promote food intake, which will lead to weight gain. In the long term, through its interaction with 5-HT$_{2C}$R, elevated Ahi1 expression will impair glucose metabolism, which will contribute to the morbidity rate of type 2 diabetes mellitus. An improved understanding of the role of Ahi1 in the metabolic side effects of antipsychotic drugs may help provide the potential target to alleviate these adverse effects.

Both pharmacological and genetic evidence implicates 5-HT$_{2C}$R as a critical receptor mediator of the effect of serotonin on feeding behavior (12, 52, 63, 64). Recent animal studies using knock-out mice have shown the 5-HT$_{2C}$R gene to be involved in the control of appetite and feeding behavior. 5-HT$_{2C}$R null mice display hyperphagia, reduced sensitivity to the anorectic effects of mCPP and dexfenfluramine, enhanced susceptibility to type 2 diabetes, and late-onset obesity syndrome (11, 12). Because 5-HT$_{2C}$R mutant mice are chronically hyperphagic from 5 weeks of age, it would be interesting to investigate whether the elevation of Ahi1 function caused by the dissociation between Ahi1 and 5-HT$_{2C}$R contributes to this phenomenon. Conditional knock-out mice strategy will help us to explore how Ahi1 influences the serotonin receptor-neuropeptide system and, subsequently, feeding and energy metabolism. Although additional studies are needed to fully characterize the neural network in which Ahi1 associates and modulates 5-HT$_{2C}$R, our findings provide a further understanding of how hypothalamic key molecules regulate feeding behavior.

REFERENCES

1. Morton, G. J., Cummings, D. E., Baskin, D. G., Barsh, G. S., and Schwartz, M. W. (2006) Central nervous system control of food intake and body weight. *Nature* **443,** 289–295
2. Sandoval, D., Cota, D., and Seeley, R. J. (2008) The integrative role of CNS fuel-sensing mechanisms in energy balance and glucose regulation. *Annu. Rev. Physiol.* **70,** 513–535
3. Jespersen, S., and Scheel-Krüger, J. (1973) Evidence for a difference in mechanism of action between fenfluramine- and amphetamine-induced anorexia. *J. Pharm. Pharmacol.* **25,** 49–54
4. Shor-Posner, G., Grinker, J. A., Marinescu, C., Brown, O., and Leibowitz, S. F. (1986) Hypothalamic serotonin in the control of meal patterns and macronutrient selection. *Brain Res. Bull.* **17,** 663–671
5. Vickers, S. P., Benwell, K. R., Porter, R. H., Bickerdike, M. J., Kennett, G. A., and Dourish, C. T. (2000) Comparative effects of continuous infusion of mCPP, Ro 60-0175, and D-fenfluramine on food intake, water intake, body weight, and locomotor activity in rats. *Br. J. Pharmacol.* **130,** 1305–1314
6. Pinder, R. M., Brogden, R. N., Sawyer, P. R., Speight, T. M., and Avery, G. S. (1975) Fenfluramine: a review of its pharmacological properties and therapeutic efficacy in obesity. *Drugs* **10,** 241–323
7. Vezzosi, D., Cartier, D., Régnier, C., Otal, P., Bennet, A., Parmentier, F., Plantavid, M., Lacroix, A., Lefebvre, H., and Caron, P. (2007) Familial adrenocorticotropin-independent macronodular adrenal hyperplasia with aberrant serotonin and vasopressin adrenal receptors. *Eur. J. Endocrinol.* **156,** 21–31
8. Kring, S. I., Werge, T., Holst, C., Toubro, S., Astrup, A., Hansen, T., Pedersen, O., and Sørensen, T. I. (2009) Polymorphisms of serotonin receptor 2A and 2C genes and COMT in relation to obesity and type 2 diabetes. *PLoS One* **4,** e6696
9. Zhou, L., Sutton, G. M., Rochford, J. J., Semple, R. K., Lam, D. D., Oksanen, L. J., Thornton-Jones, Z. D., Clifton, P. G., Yueh, C. Y., Evans, M. L., McCrimmon, R. J., Elmquist, J. K., Butler, A. A., and Heisler, L. K. (2007) Serotonin 2C receptor agonists improve type 2 diabetes via melanocortin-4 receptor signaling pathways. *Cell Metab.* **6,** 398–405
10. De Vry, J., and Schreiber, R. (2000) Effects of selected serotonin 5-HT(1) and 5-HT(2) receptor agonists on feeding behavior: possible mechanisms of action. *Neurosci. Biobehav. Rev.* **24,** 341–353
11. Nonogaki, K., Strack, A. M., Dallman, M. F., and Tecott, L. H. (1998) Leptin-independent hyperphagia and type 2 diabetes in mice with a mutated serotonin 5-HT2C receptor gene. *Nat. Med.* **4,** 1152–1156
12. Tecott, L. H., Sun, L. M., Akana, S. F., Strack, A. M., Lowenstein, D. H., Dallman, M. F., and Julius, D. (1995) Eating disorder and epilepsy in mice lacking 5-HT2c serotonin receptors. *Nature* **374,** 542–546
13. Vickers, S. P., Easton, N., Webster, L. J., Wyatt, A., Bickerdike, M. J., Dourish, C. T., and Kennett, G. A. (2003) Oral adnministration of the 5-HT2C receptor agonist, mCPP, reduces body weight gain in rats over 28 days as a result of maintained hypophagia. *Psychopharmacology* (*Berl.*) **167,** 274–280
14. Brown, C. M., and Coscina, D. V. (1995) Ineffectiveness of hypothalamic serotonin to block neuropeptide Y-induced feeding. *Pharmacol. Biochem. Behav.* **51,** 641–646
15. Heisler, L. K., Cowley, M. A., Tecott, L. H., Fan, W., Low, M. J., Smart, J. L., Rubinstein, M., Tatro, J. B., Marcus, J. N., Holstege, H., Lee, C. E., Cone, R. D., and Elmquist, J. K. (2002) Activation of central melanocortin pathways by fenfluramine. *Science* **297,** 609–611
16. Rogers, P., McKibbin, P. E., and Williams, G. (1991) Acute fenfluramine administration reduces neuropeptide Y concentrations in specific hypothalamic regions of the rat: possible implications for the anorectic effect of fenfluramine. *Peptides* **12,** 251–255
17. Poirier, Y., Kozak, C., and Jolicoeur, P. (1988) Identification of a common helper provirus integration site in Abelson murine leukemia virus-induced lymphoma DNA. *J. Virol.* **62,** 3985–3992
18. Dixon-Salazar, T., Silhavy, J. L., Marsh, S. E., Louie, C. M., Scott, L. C., Gururaj, A., Al-Gazali, L., Al-Tawari, A. A., Kayserili, H., Sztriha, L., and Gleeson, J. G. (2004) Mutations in the AHI1 gene, encoding jouberin, cause Joubert syndrome with cortical polymicrogyria. *Am. J. Hum. Genet.* **75,** 979–987
19. Utsch, B., Sayer, J. A., Attanasio, M., Pereira, R. R., Eccles, M., Hennies, H. C., Otto, E. A., and Hildebrandt, F. (2006) Identification of the first AHI1 gene mutations in nephronophthisis-associated Joubert syndrome. *Pediatr. Nephrol.* **21,** 32–35
20. Valente, E. M., Brancati, F., Silhavy, J. L., Castori, M., Marsh, S. E., Barrano, G., Bertini, E., Boltshauser, E., Zaki, M. S., Abdel-Aleem, A., Abdel-Salam, G. M., Bellacchio, E., Battini, R., Cruse, R. P., Dobyns, W. B., Krishnamoorthy, K. S., Lagier-Tourenne, C., Magee, A., Pascual-Castroviejo, I., Salpietro, C. D., Sarco, D., Dallapiccola, B., and Gleeson, J. G. (2006) AHI1 gene mutations cause specific forms of Joubert syndrome-related disorders. *Ann. Neurol.* **59,** 527–534
21. Doering, J. E., Kane, K., Hsiao, Y. C., Yao, C., Shi, B., Slowik, A. D., Dhagat, B., Scott, D. D., Ault, J. G., Page-McCaw, P. S., and Ferland, R. J. (2008) Species differences in the expression of Ahi1, a protein implicated in the neurodevelopmental disorder Joubert syndrome, with preferential accumulation to stigmoid bodies. *J. Comp. Neurol.* **511,** 238–256
22. Ferland, R. J., Eyaid, W., Collura, R. V., Tully, L. D., Hill, R. S., Al-Nouri, D., Al-Rumayyan, A., Topcu, M., Gascon, G., Bodell, A., Shugart, Y. Y., Ruvolo, M., and Walsh, C. A. (2004) Abnormal cerebellar development and axonal decussation due to mutations in AHI1 in Joubert syndrome. *Nat. Genet.* **36,** 1008–1013
23. Sheng, G., Xu, X., Lin, Y. F., Wang, C. E., Rong, J., Cheng, D., Peng, J., Jiang, X., Li, S. H., and Li, X. J. (2008) Huntingtin-associated protein 1 interacts with Ahi1 to regulate cerebellar and brainstem development in mice. *J. Clin. Invest.* **118,** 2785–2795
24. Salonen, J. T., Uimari, P., Aalto, J. M., Pirskanen, M., Kaikkonen, J., Todorova, B., Hyppönen, J., Korhonen, V. P., Asikainen, J., Devine, C., Tuomainen, T. P., Luedemann, J., Nauck, M., Kerner, W., Stephens, R. H., New, J. P., Ollier, W. E., Gibson, J. M., Payton, A., Horan, M. A., Pendleton, N., Mahoney, W., Meyre, D., Delplanque, J., Froguel, P., Luzzatto, O., Yakir, B., and Darvasi, A. (2007) Type 2 diabetes whole-genome association study in four populations: the DiaGen consortium. *Am. J. Hum. Genet.* **81,** 338–345
25. Prior, M. J., Foletta, V. C., Jowett, J. B., Segal, D. H., Carless, M. A., Curran, J. E., Dyer, T. D., Moses, E. K., McAinch, A. J., Konstantopoulos, N., Bozaoglu, K., Collier, G. R., Cameron-Smith, D., Blangero, J., and Walder, K. R. (2010) The characterization of Abelson helper integration site-1 in skeletal muscle and its links to the metabolic syndrome. *Metabolism* **59,** 1057–1064
26. Han, S. B., Choi, B. I., Lee, D., Kee, S. H., Kim, H. S., Sun, W., and Kim, H.

(2009) Regulation of AHI1 expression in adult rat brain: Implication in hypothalamic feeding control. *Biochem. Biophys. Res. Commun.* **390,** 535–540

27. Niu, S. N., Huang, Z. B., Wang, H., Rao, X. R., Kong, H., Xu, J., Li, X. J., Yang, C., and Sheng, G. Q. (2011) Brainstem Hap1-Ahi1 is involved in insulin-mediated feeding control. *FEBS Lett.* **585,** 85–91

28. Pfaffl, M. W. (2001) A new mathematical model for relative quantification in real-time RT-PCR. *Nucleic Acids Res.* **29,** e45

29. Yuan, J. S., Reed, A., Chen, F., and Stewart, C. N., Jr. (2006) Statistical analysis of real-time PCR data. *BMC Bioinformatics* **7,** 85

30. Sutton, G. M., Trevaskis, J. L., Hulver, M. W., McMillan, R. P., Markward, N. J., Babin, M. J., Meyer, E. A., and Butler, A. A. (2006) Diet-genotype interactions in the development of the obese, insulin-resistant phenotype of C57BL/6J mice lacking melanocortin-3 or -4 receptors. *Endocrinology* **147,** 2183–2196

31. Swandulla, D., and Misgeld, U. (1990) Development and properties of synaptic mechanisms in a network of rat hypothalamic neurons grown in culture. *J. Neurophysiol.* **64,** 715–726

32. Jiang, X., Hanna, Z., Kaouass, M., Girard, L., and Jolicoeur, P. (2002) Ahi-1, a novel gene encoding a modular protein with WD40-repeat and SH3 domains, is targeted by the Ahi-1 and Mis-2 provirus integrations. *J. Virol.* **76,** 9046–9059

33. Keller, L. C., Geimer, S., Romijn, E., Yates, J., 3rd, Zamora, I., and Marshall, W. F. (2009) Molecular architecture of the centriole proteome: the conserved WD40 domain protein POC1 is required for centriole duplication and length control. *Mol. Biol. Cell* **20,** 1150–1166

34. Louie, C. M., Caridi, G., Lopes, V. S., Brancati, F., Kispert, A., Lancaster, M. A., Schlossman, A. M., Otto, E. A., Leitges, M., Gröne, H. J., Lopez, I., Gudiseva, H. V., O'Toole, J. F., Vallespin, E., Ayyagari, R., Ayuso, C., Cremers, F. P., den Hollander, A. I., Koenekoop, R. K., Dallapiccola, B., Ghiggeri, G. M., Hildebrandt, F., Valente, E. M., Williams, D. S., and Gleeson, J. G. (2010) AHI1 is required for photoreceptor outer segment development and is a modifier for retinal degeneration in nephronophthisis. *Nat. Genet.* **42,** 175–180

35. Scheepers, F. E., Gespen de Wied, C. C., and Kahn, R. S. (2001) The effect of olanzapine treatment on *m*-chlorophenylpiperazine-induced hormone release in schizophrenia. *J. Clin. Psychopharmacol.* **21,** 575–582

36. Heisler, L. K., Cowley, M. A., Kishi, T., Tecott, L. H., Fan, W., Low, M. J., Smart, J. L., Rubinstein, M., Tatro, J. B., Zigman, J. M., Cone, R. D., and Elmquist, J. K. (2003) Central serotonin and melanocortin pathways regulating energy homeostasis. *Ann. N.Y. Acad. Sci.* **994,** 169–174

37. Neer, E. J., Schmidt, C. J., Nambudripad, R., and Smith, T. F. (1994) The ancient regulatory-protein family of WD-repeat proteins. *Nature* **371,** 297–300

38. Sicheri, F., Moarefi, I., and Kuriyan, J. (1997) Crystal structure of the Src family tyrosine kinase Hck. *Nature* **385,** 602–609

39. Koch, C. A., Anderson, D., Moran, M. F., Ellis, C., and Pawson, T. (1991) SH2 and SH3 domains: elements that control interactions of cytoplasmic signaling proteins. *Science* **252,** 668–674

40. Hsiao, Y. C., Tong, Z. J., Westfall, J. E., Ault, J. G., Page-McCaw, P. S., and Ferland, R. J. (2009) Ahi1, whose human ortholog is mutated in Joubert syndrome, is required for Rab8a localization, ciliogenesis and vesicle trafficking. *Hum. Mol. Genet.* **18,** 3926–3941

41. Dryden, S., McCarthy, H. D., Malabu, U. H., Ware, M., and Williams, G. (1993) Increased neuropeptide Y concentrations in specific hypothalamic nuclei of the rat following treatment with methysergide: evidence that NPY may mediate serotonin's effects on food intake. *Peptides* **14,** 791–796

42. Currie, P. J., Saxena, N., and Tu, A. Y. (1999) 5-HT(2A/2C) receptor antagonists in the paraventricular nucleus attenuate the action of DOI on NPY-stimulated eating. *Neuroreport* **10,** 3033–3036

43. Hsiao, S. H., Chung, H. H., Inui, A., Tong, Y. C., and Cheng, J. T. (2006) Inhibitory effect of 5-hydroxytryptamine on hyperphagia in mice with genetic overexpression of neuropeptide Y. *Neurosci. Lett.* **394,** 256–258

44. Boston, B. A., Blaydon, K. M., Varnerin, J., and Cone, R. D. (1997) Independent and additive effects of central POMC and leptin pathways on murine obesity. *Science* **278,** 1641–1644

45. Cone, R. D. (2005) Anatomy and regulation of the central melanocortin system. *Nat. Neurosci.* **8,** 571–578

46. Lee, Y. S., Challis, B. G., Thompson, D. A., Yeo, G. S., Keogh, J. M., Madonna, M. E., Wraight, V., Sims, M., Vatin, V., Meyre, D., Shield, J., Burren, C., Ibrahim, Z., Cheetham, T., Swift, P., Blackwood, A., Hung, C. C., Wareham, N. J., Froguel, P., Millhauser, G. L., O'Rahilly, S., and Farooqi, I. S. (2006) A POMC variant implicates beta-melanocyte-stimulating hormone in the control of human energy balance. *Cell Metab.* **3,** 135–140

47. Biebermann, H., Castañeda, T. R., van Landeghem, F., von Deimling, A., Escher, F., Brabant, G., Hebebrand, J., Hinney, A., Tschöp, M. H., Grüters, A., and Krude, H. (2006) A role for beta-melanocyte-stimulating hormone in human body-weight regulation. *Cell Metab.* **3,** 141–146

48. Fan, W., Boston, B. A., Kesterson, R. A., Hruby, V. J., and Cone, R. D. (1997) Role of melanocortinergic neurons in feeding and the agouti obesity syndrome. *Nature* **385,** 165–168

49. Adan, R. A., Cone, R. D., Burbach, J. P., and Gispen, W. H. (1994) Differential effects of melanocortin peptides on neural melanocortin receptors. *Mol. Pharmacol.* **46,** 1182–1190

50. Ollmann, M. M., Wilson, B. D., Yang, Y. K., Kerns, J. A., Chen, Y., Gantz, I., and Barsh, G. S. (1997) Antagonism of central melanocortin receptors *in vitro* and *in vivo* by agouti-related protein. *Science* **278,** 135–138

51. Stanley, B. G., and Leibowitz, S. F. (1984) Neuropeptide Y: stimulation of feeding and drinking by injection into the paraventricular nucleus. *Life Sci.* **35,** 2635–2642

52. Lam, D. D., Przydzial, M. J., Ridley, S. H., Yeo, G. S., Rochford, J. J., O'Rahilly, S., and Heisler, L. K. (2008) Serotonin 5-HT2C receptor agonist promotes hypophagia via downstream activation of melanocortin 4 receptors. *Endocrinology* **149,** 1323–1328

53. Ascher-Svanum, H., Stensland, M., Zhao, Z., and Kinon, B. J. (2005) Acute weight gain, gender, and therapeutic response to antipsychotics in the treatment of patients with schizophrenia. *BMC Psychiatry* **5,** 3

54. L'Italien, G. J., Casey, D. E., Kan, H. J., Carson, W. H., and Marcus, R. N. (2007) Comparison of metabolic syndrome incidence among schizophrenia patients treated with aripiprazole versus olanzapine or placebo. *J. Clin. Psychiatry* **68,** 1510–1516

55. Nasrallah, H. A., and Newcomer, J. W. (2004) Atypical antipsychotics and metabolic dysregulation: evaluating the risk/benefit equation and improving the standard of care. *J. Clin. Psychopharmacol.* **24,** S7–14

56. Kinon, B. J., Bassoon, B. R., Gilmore, J. A., and Tomlinson, G. D. (2001) Long-term olanzapine treatment: weight change and weight-related health factors in schizophrenia. *J. Clin. Psychiatry* **62,** 92–100

57. Nasrallah, H. (2003) A review of the effect of atypical antipsychotics on weight. *Psychoneuroendocrinology* **28,** Suppl. 1, 83–96

58. Henderson, D. C., Cagliero, E., Copeland, P. M., Borba, C. P., Evins, E., Hayden, D., Weber, M. T., Anderson, E. J., Allison, D. B., Daley, T. B., Schoenfeld, D., and Goff, D. C. (2005) Glucose metabolism in patients with schizophrenia treated with atypical antipsychotic agents: a frequently sampled intravenous glucose tolerance test and minimal model analysis. *Arch. Gen. Psychiatry* **62,** 19–28

59. Nasrallah, H. A. (2008) Atypical antipsychotic-induced metabolic side effects: insights from receptor-binding profiles. *Mol. Psychiatry* **13,** 27–35

60. Goodall, E., Oxtoby, C., Richards, R., Watkinson, G., Brown, D., and Silverstone, T. (1988) A clinical trial of the efficacy and acceptability of D-fenfluramine in the treatment of neuroleptic-induced obesity. *Br. J. Psychiatry* **153,** 208–213

61. Kennett, G. A., Whitton, P., Shah, K., and Curzon, G. (1989) Anxiogenic-like effects of mCPP and TFMPP in animal models are opposed by 5-HT1C receptor antagonists. *Eur. J. Pharmacol.* **164,** 445–454

62. Matsui-Sakata, A., Obtain, H., and Sawada, Y. (2005) Receptor occupancy-based analysis of the contributions of various receptors to antipsychotics-induced weight gain and diabetes mellitus. *Drug Metab. Pharmacokinet.* **20,** 368–378

63. Garfield, A. S., and Heisler, L. K. (2009) Pharmacological targeting of the serotonergic system for the treatment of obesity. *J. Physiol.* **587,** 49–60

64. Iordanidou, M., Tavridou, A., Vasiliadis, M. V., Arvanitidis, K. I., Petridis, J., Christakidis, D., Vargemezis, V., Bougioukas, G., and Manolopoulos, V. G. (2008) The -759C/T polymorphism of the 5-HT2C receptor is associated with type 2 diabetes in male and female Caucasians. *Pharmacogenet. Genomics* **18,** 153–159